1   **The equivalence of multi-axis spine systems:**

2   **Recommended stiffness limits using a standardized testing protocol**

3   Timothy P Holsgrove[1,2] • Dhara B Amin[3] • Sonia Ramos Pascual[2] • Boyin Ding[4] • William C

4   Welch[5] • Sabina Gheduzzi[2] • Anthony W Miles[2] • Beth A Winkelstein[5,6] • John J Costi[3]

5

6   [1]Department of Engineering, College of Engineering, Mathematics & Physical Sciences,

7   University of Exeter, Exeter, UK

8   [2]Centre for Orthopaedic Biomechanics, Department of Mechanical Engineering, University of

9   Bath, Bath, UK

10   [3]Biomechanics & Implants Research Group, The Medical Device Research Institute, Flinders

11   University, Adelaide, SA, Australia

12   [4]School of Mechanical Engineering, The University of Adelaide, Adelaide, SA, Australia

13   [5]Department of Neurosurgery, University of Pennsylvania, PA, USA

14   [6]Department of Bioengineering, School of Engineering and Applied Science, University of

15   Pennsylvania, PA, USA

16

17   **Corresponding Author**

18   Timothy P Holsgrove

19   Unit L, Innovation Building, Streatham Campus, University of Exeter, Exeter, EX4 4QF, UK

20   +44(0)1392 624682

21   t.holsgrove@exeter.ac.uk

22

1   **Abstract**

2   The complexity of multi-axis spine testing often makes it challenging to compare results from

3   different studies. The aim of this work was to develop and implement a standardized testing

4   protocol across three six-axis spine systems, compare them, and provide stiffness and phase

5   angle limits against which other test systems can be compared. Standardized synthetic lumbar

6   specimens (n=5), comprising three springs embedded in polymer at each end, were tested on

7   each system using pure moments in flexion-extension, lateral bending, and axial rotation. Tests

8   were performed using sine and triangle waves with an amplitude of 8 Nm, a frequency of 0.1 Hz,

9   and with axial preloads of 0 and 500 N. The stiffness, phase angle, and R^2 value of the moment

10   against rotation in the principal axis were calculated at the center of each specimen. The tracking

11   error was adopted as a measure of each test system to minimize non-principal loads, defined as

12   the root mean squared difference between actual and target loads. All three test systems

13   demonstrated similar stiffnesses, with small (<14%) but significant differences in 4 of 12 tests.

14   More variability was observed in the phase angle between the principal axis moment and rotation,

15   with significant differences in 10 of 12 tests. Stiffness and phase angle limits were calculated

16   based on the 95% confidence intervals from all three systems. These recommendations can be

17   used with the standard specimen and testing protocol by other research institutions to ensure

18   equivalence of different spine systems, increasing the ability to compare in-vitro spine studies.

21

Introduction

Replicating in-vivo loads in the spine is a critical aspect of in-vitro spine testing; however, the complexity of the mechanical properties of the intervertebral disc, facet joints, and the numerous muscles and ligaments that actuate and guide motion at each vertebral level make doing so a considerable challenge (Holsgrove et al., 2015b; Jaumard et al., 2011).

There are many six-axis testing systems that have been used for the biomechanical testing of the spine (Chung et al., 2002; Ding et al., 2014; Holsgrove et al., 2014; Ilharreborde et al., 2010; Kelly and Bennett, 2013; Martínez et al., 2013; Stokes et al., 2002; Wilke et al., 1994; Wilke et al., 2016), however, the designs and control capabilities of those testing systems vary considerably. Additionally, despite previous studies having demonstrated the large changes in the mechanical properties of spinal specimens due to a preload (Gardner-Morse and Stokes, 2003; Holsgrove et al., 2015a; Panjabi et al., 2001; Tawackoli et al., 2004) and the method of preload application (Cripton et al., 2000), testing rate (Costi et al., 2008; Gay et al., 2008), and testing environment (Costi et al., 2002; Pflaster et al., 1997; Wilke et al., 1998a), the standardization of in-vitro methods is still lacking, despite previous recommendations (Goel et al., 2006; Wilke et al., 1998b), which often makes it difficult, if not impossible, to compare different biomechanical studies (Holsgrove et al., 2015b).

Whilst a multi-center study has demonstrated that consistent results can be acquired in the pure moment testing of cadaveric specimens without a physiological preload (Wheeler et al., 2011), there is limited data to compare multi-axis test systems with axial preloads applied to specimens, and there is no data in regard to a standard test method with which to compare different test systems. Therefore, the aim of this study was to use existing standards (British Standards Institution, 2009, 2012), and spine testing recommendations (Goel et al., 2006; Holsgrove et al., 2015b; Wilke et al., 1998b), to develop a standard multi-axis test protocol to compare different systems, using synthetic lumbar spinal motion segments. The protocol was

1   then implemented on three systems, and the stiffness and phase angle data were used to

2   establish acceptable stiffness and phase angle limits.

3   **Materials and methods**

4   Three multi-axis testing systems were used. One custom assembly (GT1) was capable of

5   position or load control in six degrees of freedom (6DOF) using a gimbal head mounted on

6   translational axes, with a load capacity of ±500 N in shear loading, ±4000 N in axial compression-

7   tension, and ±35 Nm in all rotational axes (Holsgrove et al., 2017) (Figure 1a). Another custom

8   system (HEX) adopted a hexapod design based on the concept of the Stewart Platform, with six

9   actuators linking the base and test platforms, which was also capable of position and load control

10 in 6DOF (Lawless et al., 2014), with a load capacity of ±7.2 kN in shear, 18 kN in axial

11 compression-extension, and 1.4 kNm in all rotational axes (Figure 1b). The final system (GT2)

12 was a commercially available dual axis MTS servo-hydraulic testing machine (370.02 FlexTest

13 60; MTS Systems Corp., Eden Prairie, MN, USA) combined with an MTS kinematic spine system

14 (Bionix Spine Kinematics System; MTS Systems Corp.) to provide position or load control in four

15 axes (axial compression-tension, flexion-extension, lateral bending, and axial rotation), with a

16 custom dual platform of linear guide rails providing passive axes in anteroposterior and

17 mediolateral translation (Figure 1c). GT2 had a load capacity of 580 N in shear, 1160 N in axial

18 compression-extension, and 20 Nm in all rotational axes. However, the load cell used for the

19 control of the axial preload had a capacity of 22 kN. All three systems measured position directly

20 from sensors mounted on the system load frames.

21 After completing all tests at on each system, the tests were repeated on the original system

22 (GT1) to ensure that no damage had occurred to the specimens.

23 *Synthetic Specimen Design*

24 Six synthetic lumbar specimens were fabricated, allowing standardized comparisons to be

25 made between different multi-axis systems. The synthetic specimen design (Figure 2) was based

1   on the only international standard for pre-clinical spine testing that describes spring-based

2   anterior supports for the lumbar region of the spine, *ISO 12189:2008* (British Standards Institution,

3   2009); the dimensions and mechanical properties of the springs used for the anterior support are

4   outlined in *ISO 10243:2010+A1:2011* (British Standards Institution, 2012).

5   The criterion of *ISO 12189:2008* is limited to compression testing, where three heavy-duty die

6   cast springs of Ø25 mm and 25 mm length are placed in circular recesses within each test block.

7   However, in order to apply pure moments to the specimens, it was necessary to rigidly fix the

8   springs at each end. This was accomplished by using springs with a length of 76 mm, and

9   embedding each end in a two-part fast-curing liquid polymer (Smooth Cast® 300; Smooth-On,

10   Inc.; Macungie, PA) using a potting jig (Figure 2c) to ensure that the spacing and resulting free-

11   length was 25 mm. Each spring had a stiffness of approximately 99 N/mm but once embedded

12   with a free-length of 25 mm, the stiffness was expected to be approximately 375 N/mm (British

13   Standards Institution, 2012), giving an overall specimen compressive stiffness of approximately

14   1125 N/mm.

15   The same six polymer/spring specimens were used for testing on all three systems.

16   Additionally, the cylindrical part of the specimen pots, to which the specimens were fixed using

17   radial screws, were used for testing of the specimens to ensure consistent fixation to each test

18   system (Figure 2d).

19   *Test Regime*

20   Twelve tests (three loading directions x two waveforms x two preloads) were completed on

21   each system. Pure moments of ±8 Nm were individually applied in flexion-extension, lateral

22   bending, and axial rotation (ASTM International, 2011; Kelly and Bennett, 2013; Lawless et al.,

23   2014) to the specimens on each system according to a standardized protocol (Table 1). All axes

24   were tested first without a preload, and then with a 500 N axial preload (Costi et al., 2008; Cripton

25   et al., 2000; Holsgrove et al., 2015a), which was applied as a vertical vector. Pure moments were

1   applied using both sine and triangle waveforms for each test condition at 0.1 Hz. The time, load

2   and position data were acquired at 100 Hz for all tests. Five cycles were applied for each test,

3   with the first two cycles used for preconditioning, and the last three used for data analysis

4   (Holsgrove et al., 2015a; Holsgrove et al., 2017; Wilke et al., 1998b).

5   The coordinate system used was based on previous recommendations for spinal testing

6   (Holsgrove et al., 2015b; Wilke et al., 1998b), with the x, y, and z axes corresponding to anterior

7   shear, left lateral shear, and axial tension respectively (Figure 2d). Prior to testing, the specimen

8   pots were mounted on the test machine, and the loads were offset to zero. The specimen was

9   then fixed into the test system with the geometric center aligned along the z axis. The datum of x

10   and y axes was also adjusted to be at the geometrical center of the specimen in the GT1 and

11   HEX; the axial position of the x and y axes was not adjustable on GT2.

12   Once positioned, the test system was set to load control with a zero set point in all six axes;

13   in the case of GT2, the four active axes were operated in load control with a zero set point, and

14   the passive axes in the anteroposterior and mediolateral directions were allowed to move freely

15   to maintain minimal shear loading. The zero load condition was maintained for five minutes prior

16   to commencing pure moment tests, which were completed in the order of flexion-extension, lateral

17   bending, and axial rotation, with sine waves completed in all axes prior to the completion of

18   triangle waves. Each test of five cycles took 50 s to complete, and a one minute recovery period

19   was employed between each test. The axial preload of 500 N was then applied and equilibrated

20   with all other axes maintained in the zero load condition for five minutes prior to repeating the

21   pure moment tests using sine and triangle waves. The order of testing specimens was

22   randomized at each institution.

23   *Data Analysis*

24   The load data were adjusted to the geometrical center of the specimen using rigid body

25   transformations. Transformation matrices were calculated based on position and angle of the load

1   cell datum relative to the specimen center on each system during each test. These allowed the

2   required translations and rotations of the load matrix to be completed, and the transformed load

3   data were then used to calculate the stiffness, phase angle, R^2 value and tracking errors for each

4   test. The stiffness in the test axis was calculated over the entire load-unload period of the last

5   three cycles. Stiffness was calculated from the principal axis moment and rotation data using the

6   linear least squares method, and the R^2 value was calculated to assess the linearity. The phase

7   angle for the principal axis of each test was calculated between the input moment and measured

8   rotation for the last three cycles using the cross spectral density estimate function (Matlab: CSD.m)

9   to assess lag due to deformation of the potting material and system compliance (Amin et al., 2015;

10   Costi et al., 2008). Additionally, the ability of each system to minimize non-primary loads was

11   assessed by calculating the tracking error of the non-principal axes for each test using the mean

12   root mean squared (RMS) difference between the target and the actual load at the geometric

13   center of the specimen. The target loads were 0 N and 0 Nm except for the target axial load of

14   500 N compression during tests with a preload. The tracking error of the five non-principal axes

15   in each test were grouped into non-principal moments, shear forces, and axial force, in order to

16   provide an overall summary of the capability of each system to minimize loads. It should be noted

17   that the HEX control system completed rigid body transformations of the load data in real-time.

18   This was not possible with the GT1 and GT2 systems, so the rigid body transformations were

19   completed in post-processing, and the transformed data used for the system comparisons.

20   To ensure that the specimens had not been damaged during the tests, the stiffness and phase

21   angle of the three systems and the repeat testing on the original system were compared using

22   repeated measures ANOVAs, and in cases of significance a paired t-test post-hoc analysis with

23   Bonferroni correction was used (IBM SPSS Statistics 23.0.0.0; IBM Corporation; Armonk, NY).

24   The stiffness, phase angle, and tracking error measurements of the three systems were then

25   compared without the repeat tests using the same statistical method, and this data used to

1 compare the systems and develop the testing recommendations. All statistical analyses were

2 completed with a significance level of 0.05.

3 **Results**

4 The tests on each system demonstrated that the use of standardized synthetic specimens led

5 to a low variation in stiffness between specimens on each test system (interquartile range (IQR)

6 within 14% of the median), though one specimen was substantially lower in stiffness than other

7 specimens. That specimen had a stiffness of more than 3 times the IQR less than the median in

8 26 of the 36 tests completed (12 tests at three institutions); therefore, the specimen was regarded

9 as an outlier and was not included in the data analysis. This exclusion reduced the maximum IQR

10 across all tests to 12.4%.

11 There were no differences in the phase angle between the original tests on GT1 and the

12 repeated tests completed after testing on all three systems. There was a significant difference in

13 the stiffness of one repeated test (p=0.004 for flexion-extension, with a 500 N preload, and a

14 triangle wave), though the magnitude of change was extremely small, with a maximum change in

15 specimen stiffness of only 0.05 Nm/°. The stiffness across test systems showed good agreement

16 (Figure 3), with no significant differences between any systems without a preload, or in axial

17 rotation with a preload. There were small but significant differences in flexion-extension with a

18 preload between systems GT1 and GT2 (p=0.002 for sine waves; 0.003 for triangle waves). There

19 were also small but significant differences between all systems in lateral bending with a preload:

20 systems GT1 and GT2 (p=0.002 for sine waves; 0.003 for triangle waves); systems GT1 and HEX

21 (p=0.001 for sine waves; 0.002 for triangle waves); and systems GT2 and HEX (p=0.004 for sine

22 waves; 0.012 for triangle waves). However, whilst significant differences were detected, the

23 maximum percentage difference between systems was 13.14%, and the mean (standard

24 deviation (SD)) difference was only 5.80(3.90)%. The R^2 values of the stiffness plots

1   demonstrated that the stiffness was highly linear (Figure 4), with mean(SD) R^2 values across all

2   tests of 0.996(0.004) on GT1, 0.997(0.002) on GT2, and 0.995(0.002) on HEX.

3   The phase angle between the principal test axis moment and rotation (Figure 5) varied more

4   across systems than the stiffness, and also demonstrated differences in phase magnitude

5   between axes of the same system (Figure 5). GT1 had relatively low phase across all tests, and

6   GT2 had an extremely low phase angle in lateral bending tests. The phase was significantly

7   different between all test systems in all lateral bending tests ($p < 0.013$). In all flexion-extension

8   tests, the phase of GT1 was significantly lower than GT2 ($p < 0.012$) and HEX ($p < 0.010$), but there

9   were no differences between GT2 and HEX. In axial rotation tests with a 500 N preload, the phase

10   of GT1 was significantly lower than GT2 using sine waves ($p < 0.001$), and significantly lower than

11   GT2 and HEX using triangle waves ($p < 0.036$).

12   There were significant differences in the tracking error between at least two systems in 32 of

13   36 comparisons (Table 2), despite all systems generally maintaining loads close to target set

14   points. However, the axial tracking error was relatively high in all tests with GT2, but this was

15   particularly true in flexion-extension tests. The axial force tracking error in HEX was also relatively

16   high without a preload, and substantially higher than respective tests with an axial preload

17   (Table 2).

18   **Discussion**

19   The aim of this study was to develop and implement a standardized testing protocol to

20   compare multi-axis test systems. The synthetic lumbar spinal specimens were modified from the

21   compression only configuration of the anterior support design of ISO 12189:2008 (British

22   Standards Institution, 2009) by embedding the springs in a polymer, thus allowing a pure moment

23   protocol to be completed. Since this design was relatively simple to fabricate, it can be easily

24   adopted to assess whether other test systems are in line with the results of the present study.

25   One specimen was identified as an outlier, which may have been caused by improper potting of

the springs within the polymer. This outlier specimen was identified as the stiffness was more than three times the IQR less than the median stiffness in the majority of tests across all three systems. It is recommended that other institutions using similar specimens identify outliers using the same method.

The mean stiffness measured on the GT1 system was lower compared to GT2 and HEX without a preload, but higher with the axial preload of 500 N. This suggests that there was some system compliance without the axial load, which would also account for the increased hysteresis visible in lateral bending without a preload (Figure 4b), compared to the test with a 500 N preload (Figure 4e). The GT1 system comprises zero-backlash gears and couplings, but it is possible that there was some compliance in the gear assemblies or fixtures, which was eliminated through the application of the axial preload.

The relatively high axial load tracking error of GT2, and of HEX without a preload (Table 2) may be due to the respective load cell capacities of 22.0 kN and 18.0 kN used to control the axial load compared to that of 4.4 kN in GT1. This demonstrates that working close to the load cell capacity provides a control system advantage, though it is likely that some of the tracking error in HEX was also due to the backlash of the ball-screw actuators (Ding et al., 2015). The moving mass of HEX is also higher than the GT1 or GT2 systems, which increases the difficulty to maintain low tracking error in dynamic loading conditions, and may account for the increased magnitude and variation in the phase angle with this system (Figure 5). However, it should be noted that the phase angle results across all systems was low, with mean(SD) phase angles across all tests of 1.34(0.73)°, 2.08(1.50)°, and 2.39(0.65)° for GT1, GT2, and HEX respectively; this is result of the test specimen exhibiting elastic behavior, without the viscoelasticity or damping that would be present in a biological spine specimen. The tracking error of HEX was also higher than GT1 and GT2 in many comparisons (Table 3), and this is likely due to the system complexity, which requires that all six actuators move in order to apply movement in a single anatomical plane. However, this complexity also provides greater flexibility in applying complex loads. The tuning of

1   such systems is also a critical factor in maintaining desired loads at physiological loading rates,

2   though a variety of methods were employed in the present study: manual tuning (GT1); auto-

3   tuning (GT2); and adaptive tuning (HEX) (Lawless et al., 2014).

4   The ability to adjust the coordinate system relating to the application of loading with both GT1

5   and HEX meant that the initial center of rotation could be positioned at the geometric center of

6   the specimen. This, combined with the orientation of the load cell of GT1 being the same as the

7   specimen center, enabled the shear loads to be maintained close to the zero set point in all tests

8   on this system (Table 2). Such adjustments were not possible with GT2, leading to relatively large

9   translations of the XY platform during flexion-extension, and lateral bending tests. It is likely that

10   this altered the load transfer through the specimen, which may have contributed to the relatively

11   high axial force tracking errors in flexion-extension and lateral bending with the 500 N preload

12   compared to the same tests without a preload (Table 2).

13   The stiffness and phase results were consistent between the sine and triangle waveforms,

14   suggesting that it may not be necessary to use both waveforms in future tests that adopt the

15   standardized protocol. Sine waveforms are commonly used in spine testing to simplify test control,

16   and approximate physiologic motion (Amin et al., 2015; Chamoli et al., 2015; Costi et al., 2008;

17   Wilke et al., 2016), though triangle waves have also been adopted in position controlled tests to

18   ensure a uniform test rate (Bennett and Kelly, 2013; Gardner-Morse and Stokes, 2004; Holsgrove

19   et al., 2015a; Kotani et al., 2006). However, triangle waveforms may be less applicable in load

20   control testing where the test rate will vary according to the stiffness of the specimen.

21   A key aspect of the comparisons of the present study was to transform the loads from the load

22   cell datum to the geometric center of each specimen with a common orientation of coordinate

23   system. This is an important step due to the different designs of GT1, GT2, and HEX, and the

24   different locations of the load cell relative to the specimen. Previous studies investigating the

25   stiffness matrices of single-level spinal specimens have used similar methods to transform load

26   data to the center of the superior vertebral body (Holsgrove et al., 2015a; Stokes and Gardner-

1   Morse, 2003), but many studies do not report if any transformation was completed, and this has

2   the potential to greatly affect the results. For example, the use of a passive sub-assembly, such

3   as that of GT2, is commonly adopted in pure moment testing of spinal specimens to minimize

4   shear loading (Jaramillo et al., 2016; Kotani et al., 2006). However, the friction of a passive system,

5   or the control limitations of an active system, may result in shear forces remaining, which could

6   lead to substantial differences in the magnitude of moments at the specimen compared to the

7   load cell datum. Likewise, the effect of the preload is likely to have a substantial effect, as the

8   force of 500 N is sufficient to create considerable moments even when the lever arm of the load

9   cell datum relative to the specimen center is small. Re-analysis of the GT2 tests of the present

10   study without rigid body transformation confirms this, with a mean stiffness calculated at the load

11   cell datum of 0.55-0.70 Nm/° less in flexion-extension and lateral bending with a 500 N preload

12   compared to the stiffness at the center of the specimen.

13   The real-time load transformations on HEX were based around a fixed specimen center, which

14   was defined once the specimen was mounted. The load transformations on GT1 accounted for

15   the changes in the geometric specimen center based on axis translations during testing. Load

16   transformations from GT2 did account for changes in the position of the specimen center in the z

17   axis, but no changes in the x or y axes were accounted for, as no translational data was acquired

18   from the passive XY platform. Based on GT1 data, the changes in the geometric center during

19   testing were within 1 mm, and the stiffness based on a fixed specimen center differed by a

20   maximum of only 0.03 Nm/° across all tests. Therefore differences in a fixed/mobile specimen

21   center will not have affected the comparisons between the systems. However, changes in the

22   specimen center may have a greater effect in tests using multi-segment specimens, or tests over

23   large ranges of motion.

24   The stiffness and phase angle data from each system were used to calculate the 95 %

25   confidence intervals, which were used to produce upper and lower stiffness and phase angle

26   limits (Table 3). It is recommended that the mean stiffness and phase angle should fall within the

recommended limits in order to demonstrate test system equivalence. An increase in phase

beyond the recommended limits may suggest system compliance, low clamp-to-clamp stiffness,

or improper potting of the springs within the polymer. In such circumstances a high phase angle

would often be accompanied by a reduction in the respective stiffness. It is additionally

recommended that future studies report non-principal tracking error, in order to ensure that the

target loading parameters are suitably met. The data of the present study suggest that shear

loading can be adequately maintained within ±10 N using either the passive XY platform or active

control, and non-principal moments can generally be maintained within ±0.5 Nm.

The present study builds upon previous recommendations to standardize in-vitro spine testing

(Goel et al., 2006; Holsgrove et al., 2015b; Wilke et al., 1998b) and demonstrates that by adopting

a standardized pure moment testing protocol, the results of different multi-axis test systems can

produce consistent stiffness measurements. However, the standardization must extend not only

to the testing, but also to the rigid body transformation of loads, so that the stiffness is measured

at a common position and orientation. This approach has led to recommended stiffness and phase

angle limits measured at the center of standardized spring specimens. The testing protocol of the

present study can be adopted by other research institutions to ensure equivalence of different

multi-axis spine systems, which through the increased ability to compare in-vitro tests, will benefit

the spinal community as a whole.

Conflicts of interest

The authors declare that they have no conflicts of interest.

References

Amin, D.B., Lawless, I.M., Sommerfeld, D., Stanley, R.M., Ding, B., Costi, J.J., 2015. Effect of potting technique on the measurement of six degree-of-freedom viscoelastic properties of human lumbar spine segments. Journal of Biomechanical Engineering 137, 054501.

ASTM International, 2011. F2423-11 - Standard Guide for Functional, Kinematic, and Wear Assessment of Total Disc Prostheses. ASTM International, West Conshohocken, PA, USA.

Bennett, C.R., Kelly, B.P., 2013. Robotic application of a dynamic resultant force vector using real-time load-control: Simulation of an ideal follower load on Cadaveric L4–L5 segments. Journal of Biomechanics 46, 2087-2092.

British Standards Institution, 2009. BS ISO 12189:2008 - Implants for surgery - Mechanical testing of implantable spinal devices - Fatigue test method for spinal implant assemblies using an anterior support. British Standards Institution, London, UK.

British Standards Institution, 2012. BS ISO 10243:2010+A1:2011 - Tools for pressing - Compression springs with rectangular section - Housing dimensions and colour coding. British Standards Institution, London, UK.

Chamoli, U., Korkusuz, M.H., Sabnis, A.B., Manolescu, A.R., Tsafnat, N., Diwan, A.D., 2015. Global and segmental kinematic changes following sequential resection of posterior osteoligamentous structures in the lumbar spine: An in vitro biomechanical investigation using pure moment testing protocols. Proceedings of the Institution of Mechanical Engineers Part H-Journal of Engineering in Medicine 229, 812-821.

Chung, S.M., Teoh, S.H., Tsai, K.T., Sin, K.K., 2002. Multi-axial spine biomechanical testing system with speckle displacement instrumentation. Journal of Biomechanical Engineering 124, 471-477.

Costi, J.J., Hearn, T.C., Fazzalari, N.L., 2002. The effect of hydration on the stiffness of intervertebral discs in an ovine model. Clinical Biomechanics 17, 446-455.

1 Costi, J.J., Stokes, I.A., Gardner-Morse, M.G., Iatridis, J.C., 2008. Frequency-dependent behavior

2 of the intervertebral disc in response to each of six degree of freedom dynamic loading - Solid

3 phase and fluid phase contributions. Spine 33, 1731-1738.

4 Cripton, P.A., Bruehlmann, S.B., Orr, T.E., Oxland, T.R., Nolte, L.P., 2000. In vitro axial preload

5 application during spine flexibility testing: towards reduced apparatus-related artefacts. Journal of

6 Biomechanics 33, 1559-1568.

7 Ding, B., Cazzolato, B.S., Stanley, R.M., Grainger, S., Costi, J.J., 2014. Stiffness Analysis and

8 Control of a Stewart Platform-Based Manipulator With Decoupled Sensor–Actuator Locations for

9 Ultrahigh Accuracy Positioning Under Large External Loads. Journal of Dynamic Systems,

10 Measurement, and Control 136, 061008-061008.

11 Ding, B.Y., Cazzolato, B.S., Grainger, S., Stanley, R.M., Costi, J.J., 2015. Active preload control

12 of a redundantly actuated Stewart platform for backlash prevention. Robotics and Computer-

13 Integrated Manufacturing 32, 11-24.

14 Gardner-Morse, M.G., Stokes, I.A., 2003. Physiological axial compressive preloads increase

15 motion segment stiffness, linearity and hysteresis in all six degrees of freedom for small

16 displacements about the neutral posture. Journal of Orthopaedic Research 21, 547-552.

17 Gardner-Morse, M.G., Stokes, I.A.F., 2004. Structural behavior of human lumbar spinal motion

18 segments. Journal of Biomechanics 37, 205-212.

19 Gay, R.E., Ilharreborde, B., Zhao, K., Boumediene, E., An, K.N., 2008. The effect of loading rate

20 and degeneration on neutral region motion in human cadaveric lumbar motion segments. Clinical

21 Biomechanics 23, 1-7.

22 Goel, V.K., Panjabi, M.M., Patwardhan, A.G., Dooris, A.P., Serhan, H., 2006. Test protocols for

23 evaluation of spinal implants. Journal of Bone and Joint Surgery-American Volume 88 Suppl 2,

24 103-109.

25 Holsgrove, T.P., Gheduzzi, S., Gill, H.S., Miles, A.W., 2014. The development of a dynamic, six-

26 axis spine simulator. The Spine Journal 14, 1308-1317.

1   Holsgrove, T.P., Gill, H.S., Miles, A.W., Gheduzzi, S., 2015a. The dynamic, six-axis stiffness

2   matrix testing of porcine spinal specimens. The Spine Journal 15, 176-1884.

3   Holsgrove, T.P., Miles, A.W., Gheduzzi, S., 2017. The application of physiological loading using

4   a dynamic, multi-axis spine simulator. Medical Engineering & Physics 41, 74-80.

5   Holsgrove, T.P., Nayak, N.R., Welch, W.C., Winkelstein, B.A., 2015b. Advanced Multi-Axis Spine

6   Testing: Clinical Relevance and Research Recommendations. International Journal of Spine

7   Surgery 9, 34.

8   Ilharreborde, B., Zhao, K., Boumediene, E., Gay, R., Berglund, L., An, K.N., 2010. A dynamic

9   method for in vitro multisegment spine testing. Orthopaedics & Traumatology: Surgery &

10   Research 96, 456-461.

11   Jaramillo, H.E., Puttlitz, C.M., McGilvray, K., Garcia, J.J., 2016. Characterization of the L4-L5-S1

12   motion segment using the stepwise reduction method. Journal of Biomechanics 49, 1248-1254.

13   Jaumard, N.V., Welch, W.C., Winkelstein, B.A., 2011. Spinal Facet Joint Biomechanics and

14   Mechanotransduction in Normal, Injury and Degenerative Conditions. Journal of Biomechanical

15   Engineering 133, 071010-071010.

16   Kelly, B.P., Bennett, C.R., 2013. Design and validation of a novel Cartesian biomechanical testing

17   system with coordinated 6DOF real-time load control: application to the lumbar spine (L1–S, L4–

18   L5). Journal of Biomechanics 46, 1948-1954.

19   Kotani, Y., Cunningham, B.W., Abumi, K., Dmitriev, A.E., Hu, N.B., Ito, M., Shikinami, Y., McAfee,

20   P.C., Minami, A., 2006. Multidirectional flexibility analysis of anterior and posterior lumbar artificial

21   disc reconstruction: in vitro human cadaveric spine model. European Spine Journal 15, 1511-

22   1520.

23   Lawless, I.M., Ding, B., Cazzolato, B.S., Costi, J.J., 2014. Adaptive velocity-based six degree of

24   freedom load control for real-time unconstrained biomechanical testing. Journal of Biomechanics

25   47, 3241-3247.

1 Martínez, H., Obst, T., Ulbrich, H., Burgkart, R., 2013. A novel application of direct force control

2 to perform in-vitro biomechanical tests using robotic technology. Journal of Biomechanics 46,

3 1379-1382.

4 Panjabi, M.M., Miura, T., Cripton, P.A., Wang, J.L., Nain, A.S., DuBois, C., 2001. Development of

5 a system for in vitro neck muscle force replication in whole cervical spine experiments. Spine 26,

6 2214-2219.

7 Pflaster, D.S., Krag, M.H., Johnson, C.C., Haugh, L.D., Pope, M.H., 1997. Effect of test

8 environment on intervertebral disc hydration. Spine 22, 133-139.

9 Stokes, I.A., Gardner-Morse, M., Churchill, D., Laible, J.P., 2002. Measurement of a spinal motion

10 segment stiffness matrix. Journal of Biomechanics 35, 517-521.

11 Stokes, I.A.F., Gardner-Morse, M., 2003. Spinal stiffness increases with axial load: another

12 stabilizing consequence of muscle action. Journal of Electromyography and Kinesiology 13, 397-

13 402.

14 Tawackoli, W., Marco, R., Liebschner, M.A., 2004. The effect of compressive axial preload on the

15 flexibility of the thoracolumbar spine. Spine 29, 988-993.

16 Wheeler, D.J., Freeman, A.L., Ellingson, A.M., Nuckley, D.J., Buckley, J.M., Scheer, J.K.,

17 Crawford, N.R., Bechtold, J.E., 2011. Inter-laboratory variability in in vitro spinal segment flexibility

18 testing. Journal of Biomechanics 44, 2383-2387.

19 Wilke, H.J., Claes, L., Schmitt, H., Wolf, S., 1994. A universal spine tester for in vitro experiments

20 with muscle force simulation. European Spine Journal 3, 91-97.

21 Wilke, H.J., Jungkunz, B., Wenger, K., Claes, L.E., 1998a. Spinal segment range of motion as a

22 function of in vitro test conditions: effects of exposure period, accumulated cycles, angular-

23 deformation rate, and moisture condition. The Anatomical Record 251, 15-19.

24 Wilke, H.J., Kienle, A., Maile, S., Rasche, V., Berger-Roscher, N., 2016. A new dynamic six

25 degrees of freedom disc-loading simulator allows to provoke disc damage and herniation.

26 European Spine Journal 25, 1363-1372.

1 Wilke, H.J., Wenger, K., Claes, L., 1998b. Testing criteria for spinal implants: recommendations

2 for the standardization of in vitro stability testing of spinal implants. European Spine Journal 7,

3 148-154.

4

5
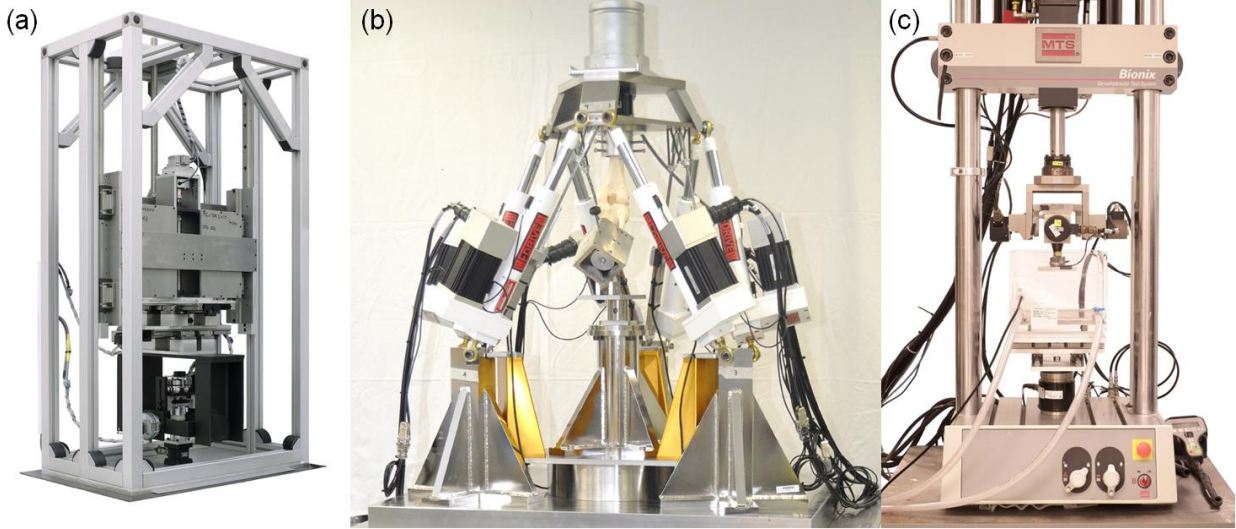
Figure 1. The three multi-axis test systems of the present study. A custom system (GT1) comprising a gimbal and translation platform capable of 6DOF position or load control (a). A custom hexapod system (HEX) with six actuators linking the base and test platforms to provide 6DOF position or load control (b). A commercial servo-hydraulic test system (GT2) capable of position or load control in four axes, with a custom passive platform to minimize anteroposterior and mediolateral shear loads (c).

1

(a)

(b)

SECTION AA

(c)

Potting jig

(d)

Superior specimen pot

Inferior specimen pot

2
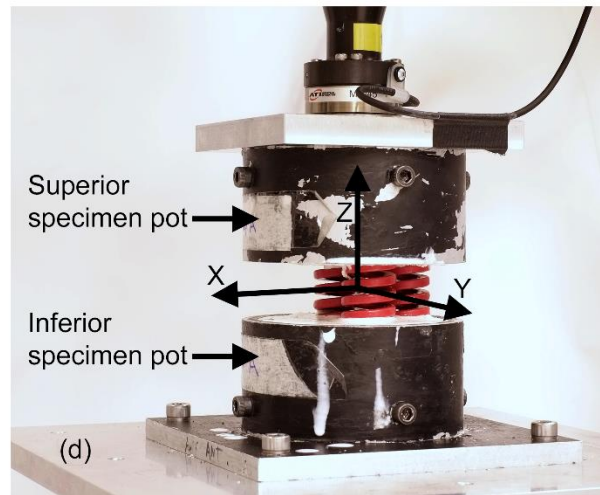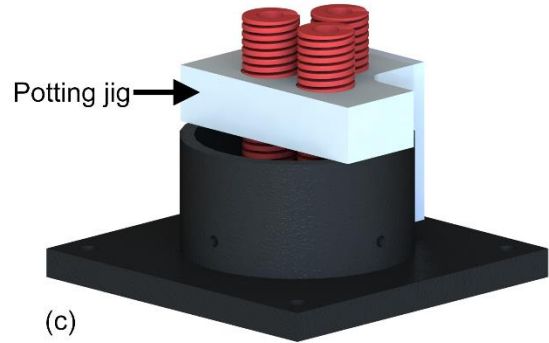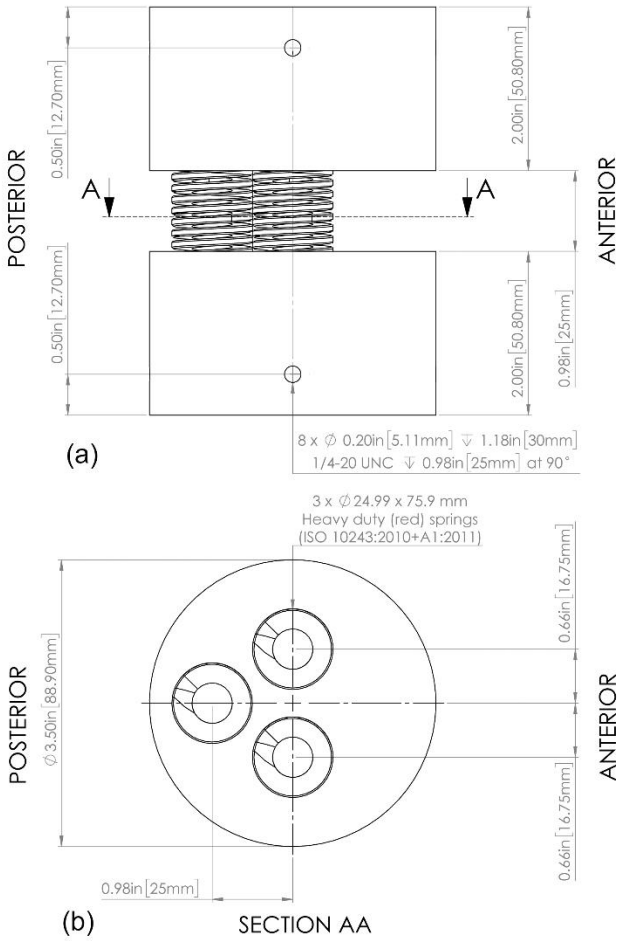
Figure 2. Spring spacing of the synthetic lumbar specimens based on ISO 12189:2008 in the lateral view (a), and an axial cross-section AA (b).Schematic of the springs arranged for standardized potting in fast-curing polymer using a jig (c). A potted specimen mounted on a test system with the coordinate system denoted (d).
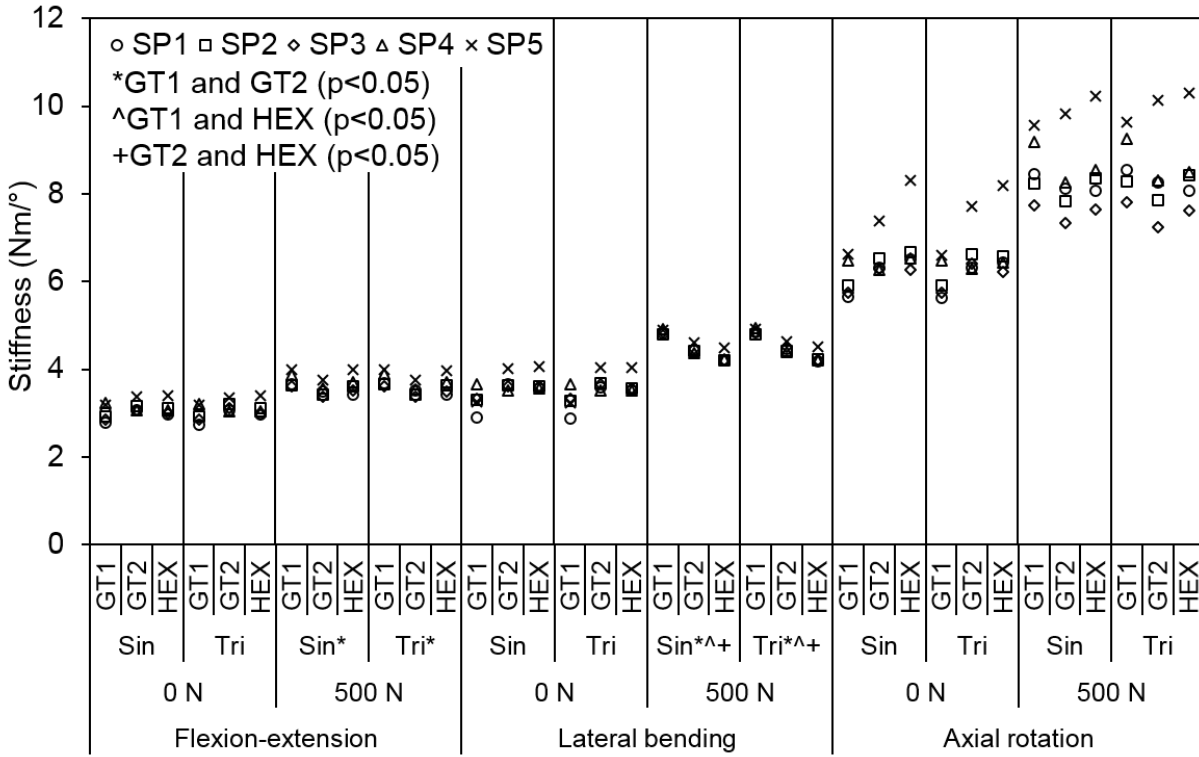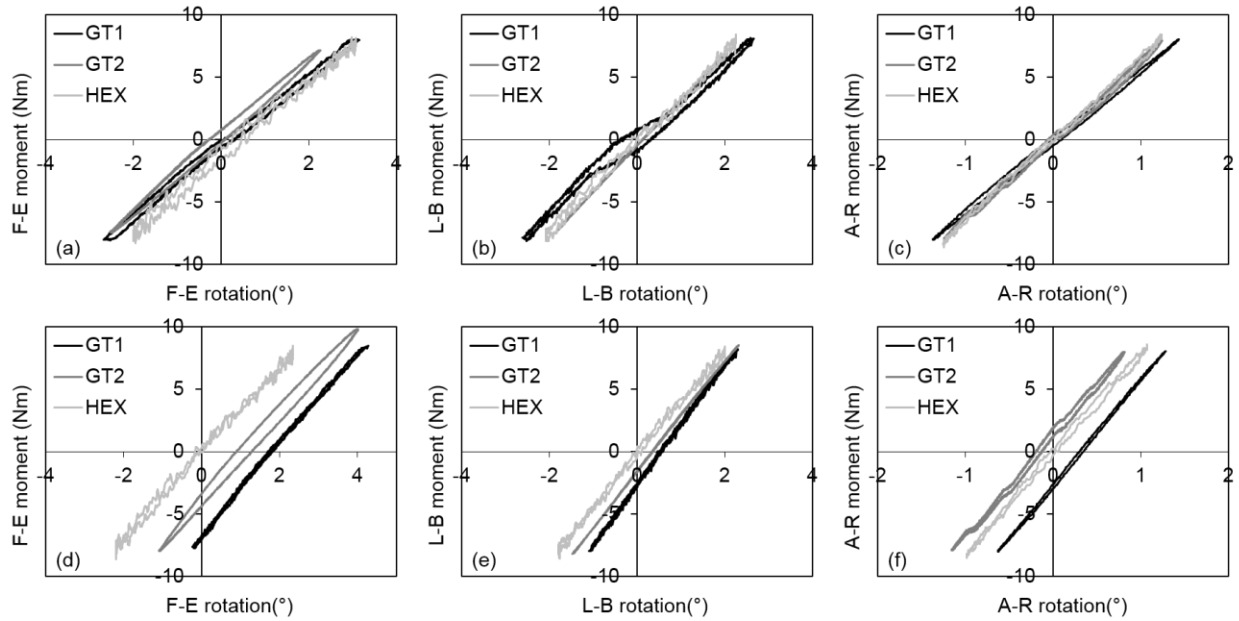
Figure 3. Stiffness of each specimen (n=5) in flexion-extension, lateral bending, and axial rotation tests with a 0 N and 500 N preload using sine and triangle waveforms on three different test systems (GT1, GT2, and HEX). Statistical significance (p<0.05) is denoted for comparisons between each system for each test condition: *GT1 and GT2; ^GT1 and HEX; +GT2 and HEX.

1

Figure 4. Moment against rotation plots of a single specimen using a sine wave profile on each test system (GT1, GT2, and HEX) measured at the geometric center of the specimen with an axial preload of 0 N in flexion-extension (a), lateral bending (b), and axial rotation (c), and with an axial preload of 500 N in flexion-extension (d), lateral bending (e), and axial rotation (f).

Figure 5. Phase between the principal test axis rotation and moment for each specimen (n=5) in flexion-extension, lateral bending, and axial rotation tests with a 0 and 500 N pr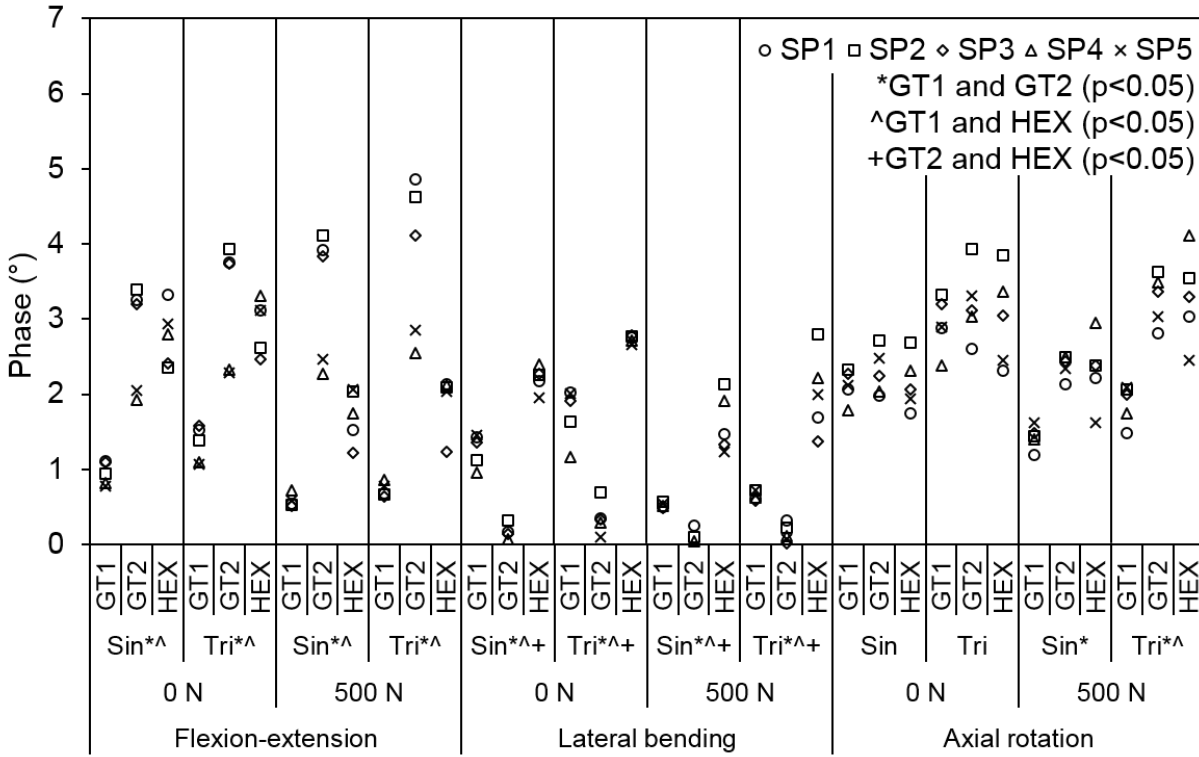eload using sine and triangle waveforms on three different test systems (GT1, GT2, and HEX). Statistical significance (p<0.05) is denoted for comparisons between each system for each test condition: *GT1 and GT2; ^GT1 and HEX; +GT2 and HEX.

1   **Table 1**. The standardized pure moment testing protocol

Step	Description
1	Mount specimen pots into the test system.
2	Offset all loads to zero.
3	Rigidly fix the specimen into the specimen pots.
4	Adjust the position to minimize the loads in all axes.
5	Offset all positions to zero.
6	Change all active axes to load control with a zero set point.
7	Five-minute equilibration period.
8	Five, 0.1 Hz sine wave cycles of ±8 Nm in flexion-extension.
9	One-minute recovery period.
10	Five, 0.1 Hz sine waves of ±8 Nm in lateral bending.
11	One-minute recovery period.
12	Five, 0.1 Hz sine waves of ±8 Nm in axial rotation.
13	One-minute recovery period.
14	Five, 0.1 Hz triangle waves of ±8 Nm in flexion-extension.
15	One-minute recovery period.
16	Five, 0.1 Hz triangle waves of ±8 Nm in lateral bending.
17	One-minute recovery period.
18	Five, 0.1 Hz triangle waves of ±8 Nm in axial rotation.
19	Change the axial load set point to 500 N of compression.
20	Five-minute equilibration period.
21	Repeat steps 8-18.
22	Return axial load set point to 0 N.
23	Change all active axes to position control.
24	Remove the specimen.
25	Repeat steps 3-24 for all other specimens.

2

Table 2. The mean(SD) RMS tracking error of non-principal moments, shear forces, and axial force for each system in flexion-extension,

2   lateral bending, and axial rotation. Statistical significance (p<0.05) is denoted for comparisons between each system for each test

3   condition: *GT1 and GT2; ^GT1 and HEX; +GT2 and HEX.

	Non-principal moments (Nm)											
	Flexion-extension				Lateral bending				Axial rotation			
	0 N		500 N		0 N		500 N		0 N		500 N	
System	Sin*^+	Tri*^	Sin^	Tri	Sin*^+	Tri*^+	Sin*^+	Tri	Sin*^	Tri*^+	Sin*^	Tri
GT1	0.10(0.01)	0.09(0.01)	0.12(0.02)	0.13(0.02)	0.08(0.00)	0.07(0.00)	0.19(0.01)	0.19(0.01)	0.09(0.01)	0.09(0.01)	0.25(0.00)	0.25(0.00)
GT2	0.19(0.06)	0.22(0.02)	0.21(0.09)	0.19(0.08)	0.19(0.04)	0.20(0.04)	0.41(0.09)	0.40(0.14)	0.40(0.09)	0.48(0.04)	0.57(0.19)	0.61(0.28)
HEX	0.29(0.02)	0.27(0.03)	0.27(0.02)	0.25(0.03)	0.31(0.04)	0.29(0.02)	0.32(0.04)	0.32(0.03)	0.29(0.01)	0.28(0.01)	0.36(0.03)	0.35(0.03)
	Shear forces (N)											
	Flexion-extension				Lateral bending				Axial rotation			
	0 N		500 N		0 N		500 N		0 N		500 N	
System	Sin*^	Tri*^+	Sin*^	Tri*^+	Sin*^+	Tri*^+	Sin*^+	Tri*^+	Sin*^+	Tri*^+	Sin*^+	Tri*^+
GT1	0.58(0.04)	0.58(0.04)	0.63(0.03)	0.65(0.03)	0.62(0.06)	0.61(0.05)	0.60(0.04)	0.61(0.03)	0.55(0.04)	0.54(0.01)	0.58(0.04)	0.57(0.03)
GT2	5.92(0.79)	6.47(0.24)	6.09(1.02)	6.19(0.88)	6.36(0.48)	6.75(0.45)	6.33(0.22)	6.45(0.71)	5.31(1.19)	6.24(0.52)	3.82(0.88)	4.24(0.57)
HEX	7.65(1.82)	7.48(1.46)	7.92(0.69)	8.20(1.03)	8.22(1.87)	8.26(1.59)	10.9(1.75)	10.4(2.37)	8.49(0.86)	8.88(0.75)	9.67(1.53)	9.77(2.38)
	Axial force (N)											
	Flexion-extension				Lateral bending				Axial rotation			
	0 N		500 N		0 N		500 N		0 N		500 N	
System	Sin*^	Tri*^	Sin*+	Tri*+	Sin^	Tri*^	Sin*+	Tri*^+	Sin*^	Tri*^	Sin*^+	Tri
GT1	1.93(0.07)	1.86(0.08)	1.68(0.05)	1.70(0.08)	1.60(0.08)	1.47(0.04)	1.27(0.04)	1.31(0.03)	1.38(0.10)	1.33(0.08)	1.36(0.04)	1.37(0.03)
GT2	36.4(12.7)	39.5(15.7)	51.0(11.9)	51.6(19.9)	16.1(11.8)	22.2(13.6)	37.4(24.9)	36.6(22.0)	22.1(13.9)	44.8(27.2)	28.6(11.6)	28.2(26.9)
HEX	57.4(4.78)	49.4(3.81)	2.30(0.36)	2.27(0.32)	24.4(12.4)	21.5(10.8)	1.14(0.29)	0.98(0.53)	27.6(3.18)	25.0(2.75)	0.30(0.17)	0.27(0.09)

4

1   **Table 3.** Recommended stiffness and phase limits based on the 95 % confidence intervals of

2   tests across all three systems of the present study.

Parameter	0 N preload					
	FE		LB		AR	
	Sin	Tri	Sin	Tri	Sin	Tri
Stiffness upper limit (Nm/°)	3.26	3.26	3.87	3.87	7.57	7.47
Stiffness lower limit (Nm/°)	2.82	2.80	3.05	3.03	5.70	5.68
Phase upper limit (°)	3.39	3.93	2.35	2.78	2.56	3.63
Phase lower limit (°)	0.82	1.12	0.02	0.17	1.83	2.45
	500 N axial preload					
	FE		LB		AR	
	Sin	Tri	Sin	Tri	Sin	Tri
Stiffness upper limit (Nm/°)	3.90	3.91	4.90	4.91	9.43	9.47
Stiffness lower limit (Nm/°)	3.38	3.39	4.15	4.14	7.45	7.41
Phase upper limit (°)	4.09	4.72	1.96	2.49	2.73	3.82
Phase lower limit (°)	0.50	0.64	0.00	0.04	1.29	1.65

3